Binding of Aflatoxin B₁ Metabolites in Extrahepatic Tissues in Fetal and Infant Mice and in Adult Mice with Depleted Glutathione Levels[1]

Pia Larsson[2] and Hans Tjälve

Department of Pharmacology and Toxicology, Faculty of Veterinary Medicine, Swedish University of Agricultural Sciences, BMC, Box 573, S-751 23 Uppsala, Sweden

ABSTRACT

Whole-body autoradiography of ^{3}H-labeled aflatoxin B₁ (AFB₁) in adult C57BL mice pretreated with the glutathione (GSH)-depleting agent phorone showed accumulation of tissue-bound radioactivity in the nasal olfactory and respiratory mucosa, the mucosa of the nasopharyngeal duct, and the tracheal and esophageal mucosa, which was not seen in unpretreated adult mice. The altered distribution pictures induced by the phorone are probably related to decreased tissue levels of GSH. The AFB₁ is likely to be bioactivated locally in the extrahepatic tissues; in nonpretreated mice the reactive AFB₁ metabolite formed is probably scavenged by GSH via the action of glutathione-S-transferase, whereas in the mice with depleted GSH levels a binding to tissue macromolecules will instead take place. The mechanism indicated above is supported by results of *in vitro* experiments in which the nasal olfactory mucosa and the esophageal mucosa were shown to have a capacity to form tissue-bound ^{3}H-AFB₁ metabolites. This formation was decreased when the incubations were performed in the presence of GSH. In addition, the treatments of mice with phorone were shown to induce a strong GSH depletion in the nasal olfactory mucosa and the esophageal mucosa.

In autoradiographic studies performed with 1- and 5-day-old infant mice a marked localization of bound ^{3}H-AFB₁ metabolites was found in the nasal olfactory mucosa, and in the 5-day-old infant there was also a labeling of the mucosa of the nasopharyngeal duct, the pharyngeal and esophageal mucosa, and the tracheal mucosa. Experiments *in vitro* with the nasal olfactory mucosa of 5-day-old infants demonstrated a marked binding of ^{3}H-AFB₁ metabolites in this tissue. Incubations together with GSH decreased this binding, although the inhibition was less marked than in the adult animal. The *in vivo* accumulation of bound AFB₁ metabolites in the extrahepatic tissues of the infant mice may be related to low glutathione-S-transferase (GST) activity in the tissues of the young animals. In addition, some extrahepatic tissues may have a considerable capacity to bioactivate the AFB₁ at early age.

Autoradiography of ^{3}H-AFB₁ in pregnant mice showed a labeling of the fetal nasal olfactory mucosa at day 18 but not at day 14 of gestation. This indicates that AFB₁-bioactivating enzymes develop in the fetal nasal olfactory mucosa in late gestation.

INTRODUCTION

AFB₁[3] is a highly potent hepatotoxin and hepatocarcinogen produced by *Aspergillus flavus* and *Aspergillus parasiticus*. AFB₁ requires activation by cytochrome P-450 enzymes to form a reactive electrophile, the 8,9-epoxide of AFB₁, which binds to proteins and DNA (1–3). The AFB₁-8,9-epoxide may also bind to GSH, via the action of GST (4–6). AFB₁-8,9-dihydrodiol can in addition be formed from the epoxide, spontaneously or via the action of epoxide hydrolase (7, 8). The binding to GSH is an important inactivation pathway, whereas the formation of the AFB₁-8,9-dihydrodiol usually appears to be of minor importance (9). Species vary greatly in their sensitivity to AFB₁ toxicity, which in part may be related to their ability to bioactivate the mycotoxin but also may be dependent on their capacities to detoxify the reactive metabolite.

Mice are markedly refractory to the negative effects of AFB₁. This may be related to a high capacity of the liver to form GSH conjugates resulting in a rapid excretion of a large proportion of the administered AFB₁ dose (9, 10). It has been reported that the mouse liver contains a GST isoenzyme, which exhibits high activity towards the AFB₁-8,9-epoxide (11, 12). Nonenzymatic reactions of the epoxide with GSH have been shown to be negligible (4).

In infant mice, the GST activity in the liver toward a number of different substrates has been shown to be lower than in adult mice (13). This implies that reactive metabolites of xenobiotics may be more prone to bind to tissue macromolecules in young as compared to adult mice. On the other hand, the bioactivating enzyme systems may not be developed in the young animals to the same extent as in the adults, which may lead to production of only small quantities of the reactive metabolites.

We have recently examined the tissue disposition of ^{3}H-AFB₁ in adult mice by autoradiographic techniques (14). Marked formation of tissue-bound metabolites was seen in the liver and in addition in some nasal glands. The nasal glands also had a capacity to metabolize the ^{3}H-AFB₁ *in vitro*. In the present study, autoradiography has been used to examine the disposition of ^{3}H-AFB₁ in adult mice in which the GSH levels have been decreased by pretreatments with phorone. The disposition of the ^{3}H-AFB₁ has also been examined in young mice. In addition, the labeling of fetal tissues was examined by autoradiography in pregnant mice given injections of ^{3}H-AFB₁.

The autoradiographic results showed the appearance of bound AFB₁ metabolites in the nasal olfactory mucosa, the upper respiratory pathways, and the esophagus of the phorone-pretreated adult mice. These tissues were also labeled in young mice. Experiments were then performed *in vitro* in which we examined the capacity of the nasal olfactory mucosa and the esophageal mucosa to form tissue-bound AFB₁ metabolites. Comparative experiments were performed with the liver.

MATERIALS AND METHODS

Chemicals. ^{3}H-AFB₁ with a specific radioactivity of 15 Ci/mmol was purchased from Moravek Biochemicals (Brea, CA). Nonlabeled AFB₁ and GSH were obtained from Sigma (St. Louis, MO). Phorone was obtained from Aldrich (Steinheim, Germany). Metyrapone was a gift from Ciba-Geigy (Basel, Switzerland). Other chemicals used in the study were of analytical grade and obtained from regular commercial sources.

Animals. Male and nonpregnant and pregnant female C57Bl-mice were obtained from Alab (Uppsala, Sweden). The infants of the pregnant mice were used on days 1 and 5 after birth. The mice were given a standard pellet diet (Ewos AB, Södertälje, Sweden) and tap water *ad libitum*. To obtain pregnant animals for the whole-body autoradiography, mice were mated overnight. The next morning, the females were

checked for vaginal plugs. This day was considered as day 1 of pregnancy.

Whole-Body Autoradiography. Two female nonpregnant mice were pretreated i.p. with phorone (250 mg/kg dissolved in 0.2 ml corn oil) 90 min before s.c. injections in the neck of ^{3}H-AFB₁. One mouse received a dose of 80 μg AFB₁/kg body weight and the other received 8 mg AFB₁/kg body weight. The ^{3}H-AFB₁ was dissolved in 25 μl of 50% ethanol. For both dose levels 4 μCi ^{3}H-AFB₁/g body weight served as tracer. Two control mice were given injections of ^{3}H-AFB₁ as above but without phorone pretreatment. All mice were killed 1 h after the ^{3}H-AFB₁ injections.

One- and 5-day-old infant mice were given s.c. injections (in the neck) of ^{3}H-AFB₁ (4 μCi/g, 80 μg/kg body weight) dissolved in 4 μl 50% ethanol and were killed 1 h after the injections.

One pregnant mouse on day 14 of gestation and two pregnant mice on day 18 of gestation were given i.v. injections of ^{3}H-AFB₁ in a tail vein (2 μCi/g body weight, 42 μg/kg body weight) dissolved in 20 μl ethanol. The 14-day-pregnant mouse was killed after 1 h. The 18-day-pregnant mice were killed after 1 and 4 h, respectively.

All animals were killed in a CO_2 atmosphere, embedded in aqueous carboxymethylcellulose, and sectioned for whole-body autoradiography as described by Ullberg (15).

To study the distribution of firmly bound radioactivity, every other freeze-dried tissue section was extracted successively with 5% trichloroacetic acid, 50% ethanol, 99.5% ethanol, and heptane for 1 min, and then rinsed with tap water for 5 min. The sections were dried and pressed against X-ray films (Ultrofilm; LKB, Bromma, Sweden) together with the adjacent nonextracted sections.

Microautoradiography. Microautoradiography was performed with tissues obtained from a 5-day-old mouse given an injection of ^{3}H-AFB₁, and with tissue pieces from nonpretreated adult and 5-day-old mice incubated with ^{3}H-AFB₁.

The 5-day-old mouse was given an injection of ^{3}H-AFB₁ s.c. (15 μCi/ g; 300 μg/kg body weight) and killed after 1 h. Pieces of the nose, the esophagus, and the trachea were removed and fixed in 4% formaldehyde in phosphate buffer, pH 7.4.

In the in vitro experiments, nasal tissues from nontreated 5-day-old and adult female mice were removed and incubated with 2 μCi ^{3}H-AFB₁ (0.07 μM) under O_2 atmosphere for 1 h at 37°C. The incubation media consisted of 50 mM phosphate buffer, pH 7.4, containing 3 mM MgCl₂, 60 mM KCl, 0.4 mM NADP, and 3 mM glucose 6-phosphate. The total volume was 2.0 ml. After the incubation, the pieces were fixed in 4% formaldehyde in phosphate buffer, pH 7.4.

The fixed tissues obtained from the ^{3}H-AFB₁-injected mouse and the tissues incubated with ^{3}H-AFB₁ were dehydrated in an ethanol series and embedded in Historesin (LKB-Produkter, Bromma, Sweden). Two-μm-thick sections were cut on glass slides and covered with Kodak NTB emulsion. The sections were stained with hematoxylin-eosin or according to the periodic acid-Schiff technique as described earlier (14). Exposure was carried out for 3 weeks at 4°C, followed by photographic development and fixation.

The histological fixation and embedding procedure included the following media and time intervals: 4% formaldehyde, 4 days; 70% ethanol, 1 h, twice; 95% ethanol, 1 h, twice; 99.6% ethanol, 30 min, twice; Historesin, overnight. Aliquots of the various media were taken and checked for radioactivity contents. It was found that a high proportion of the tissue radioactivity was released into the formaldehyde solution. A low radioactivity was detected in the 70% ethanol and an even lower amount in the 95% ethanol. No radioactivity could be detected in the 99.6% ethanol or the Historesin. Thus, the fixation and embedding procedures will remove unbound metabolites and the autoradiograms will, therefore, show only tissue-bound radioactivity.

Autoradiography of the Esophagus Incubated with ^{3}H-AFB₁. Esophagi of nonpretreated female mice were incubated with ^{3}H-AFB₁ (2 μCi/ incubation, 0.07 μM) for 1 h at 37°C in incubation media of the composition described above (see "Microautoradiography"). In the incubations O_2, N_2, or CO were used as atmospheres. In one incubation, in which O_2 was used as atmosphere, the cytochrome P-450 inhibitor metyrapone (0.5 mM in the solution) was also added to the medium. After the incubations, the tissues were rinsed for 1 min in physiological

saline and used for autoradiography with dried or extracted tape sections, as described above (see "Whole-Body Autoradiography").

Formation of Protein-bound Metabolites from ^{3}H-AFB₁ by S-9 Preparations of the Nasal Olfactory Mucosa, the Esophageal Mucosa, and the Liver. Nonpretreated female adult and 5-day-old mice were killed in CO_2 atmosphere. In the adult animals, the nasal olfactory mucosa, the esophageal mucosa, and the liver were excised, whereas in the young animals only the nasal olfactory mucosa and the liver were taken. The nasal olfactory mucosa and the esophageal mucosa were prepared under a dissection microscope. The nasal olfactory epithelium is distinguished by its brownish color and can be made free from bone and cartilage of the turbinates and the septum. The esophageal mucosa was stripped off the other tissue layers after the lumen had been opened with a longitudinal incision with a pair of scissors. The tissues were sliced and homogenized in a Potter-Elvehjem homogenizor in ice-cold 0.02 M Tris-HCl-1.15% KCl buffer, pH 7.4. The combined tissues from 15 adult mice or 30 infants were used for the nasal olfactory mucosa; for the esophagus, combined tissues from 20 adult mice were used; for the liver, combined tissues from 8 adult mice or 20 infants were used. The homogenates were centrifuged at 9000 × g for 25 min at 4°C. The resulting supernatants, the S-9 preparations, were then collected and stored at −70°C until used.

The formation of protein-bound metabolites from ^{3}H-AFB₁ was determined in incubations with the S-9 preparations. The total volume of each incubation was 1.0 ml. The incubations medium was O_2-saturated 50 mM phosphate buffer, pH 7.4, containing 3 mM MgCl₂, 60 mM KCl, 3 mM glucose-6-phosphate, 0.4 mM NADP and 1 unit/ml of glucose-6-phosphate dehydrogenase. Various amounts of S-9 preparations, corresponding to 0.1–0.6 mg of protein, were added to the incubations. ^{3}H-AFB₁ (0.2 μCi) was added to each incubation together with nonlabeled AFB₁ to obtain the desired concentrations of the mycotoxin.

In a separate experiment the effect of GSH (5 mM) in the incubation media on the formation of protein-bound metabolites by the liver, the nasal olfactory mucosa, and the esophageal mucosa from adults and by the nasal olfactory mucosa and the liver from 5-day-old mice was examined.

In a further experiment, the effect of 0.5 mM metyrapone in the incubation media on the formation of protein-bound metabolites by the nasal olfactory mucosa and the liver was examined. Incubations were performed for 20 min, with 0.25 mg S-9 protein and 0.08 μM ^{3}H-AFB₁.

At the end of the incubations the metabolic reactions were stopped by adding 1 ml of ice-cold methanol. The protein-fraction was extracted using the method of Baker and Van Dyke (16). In the procedure, the precipitate was first extracted with 2 ml of chloroform. Then, repeated solubilizations of the protein pellet in 1 ml of 1% sodium dodecyl sulfate and precipitations in 5 ml of acetone were performed. The procedure was continued until no more radioactivity was removed from the protein precipitates. After this, the precipitates were solubilized by adding 1 ml of 1 M NaOH. Aliquots were taken for liquid scintillation counting, using 10 ml of Hionic-Fluor as scintillation fluid, and for protein determination according to the method of Lowry et al. (17).

Determination of NPSH. Two groups of 6 adult female mice were given i.p. injections of phorone (250 mg/kg body weight) in 0.2 ml corn oil. Two groups of 6 adult mice which served as controls were given only corn oil. The mice were killed in CO_2 atmosphere 2 h after the injection. The nasal olfactory mucosa, the esophageal mucosa, and the liver from each group were pooled and the GSH level was determined according to the NPSH method of Sedlak and Lindsay (18).

Statistical Analysis. Statistical significances were judged with the two-tailed Student t test for differences between mean values.

RESULTS

Whole-Body Autoradiography. Whole-body autoradiography of freeze-dried tissue sections of the adult mice killed 1 h after the injection of ^{3}H-AFB₁ showed a high labeling of the blood. In the liver, the radioactivity markedly exceeded the level of the

blood. High radioactivity was present in the bile ducts, the gallbladder, the kidneys, the urine, and the contents of the small intestine. There was also a high radioactivity in the melanin of the eye and the skin. In the nose, there was a considerable radioactivity in the lateral nasal gland (Steno's gland) and some serous glands in the respiratory region (Fig. 1A). In autoradi-

ograms of extracted tissue sections of these mice, marked radioactivity was retained only in the liver and the nasal glands (Fig. 1B). Similar distribution pictures were seen in the mice given injections of the low and high doses of the ^{3}H-AFB₁.

The distribution patterns seen in the mice pretreated with phorone were similar in most aspects to those seen in the
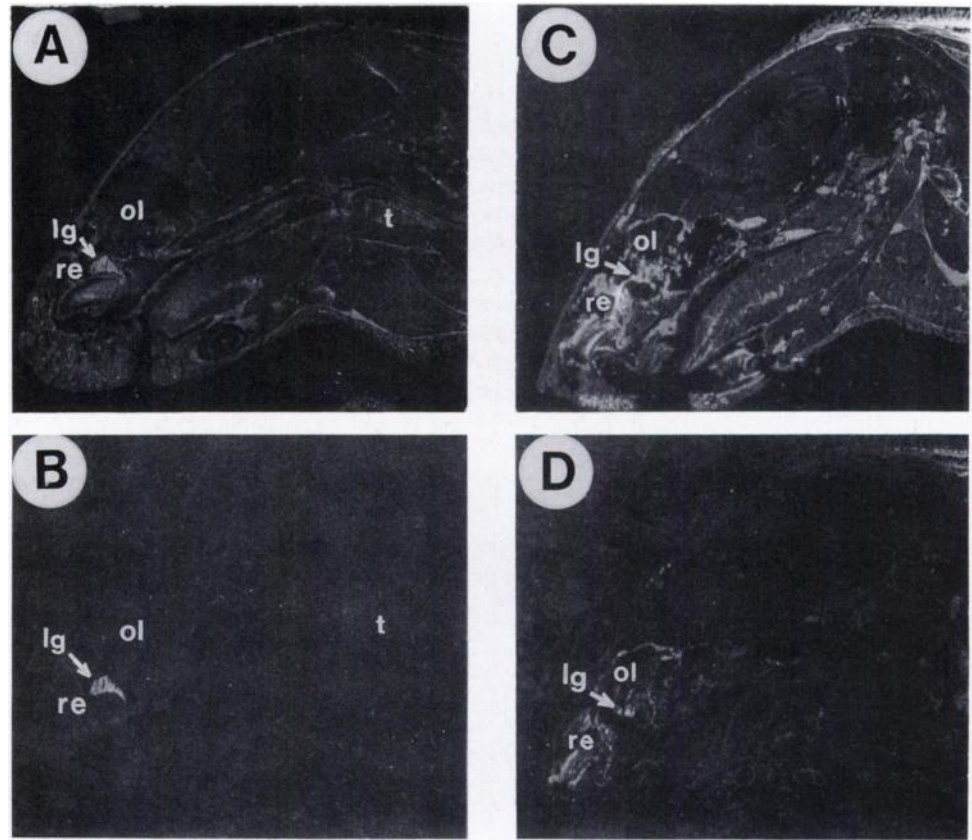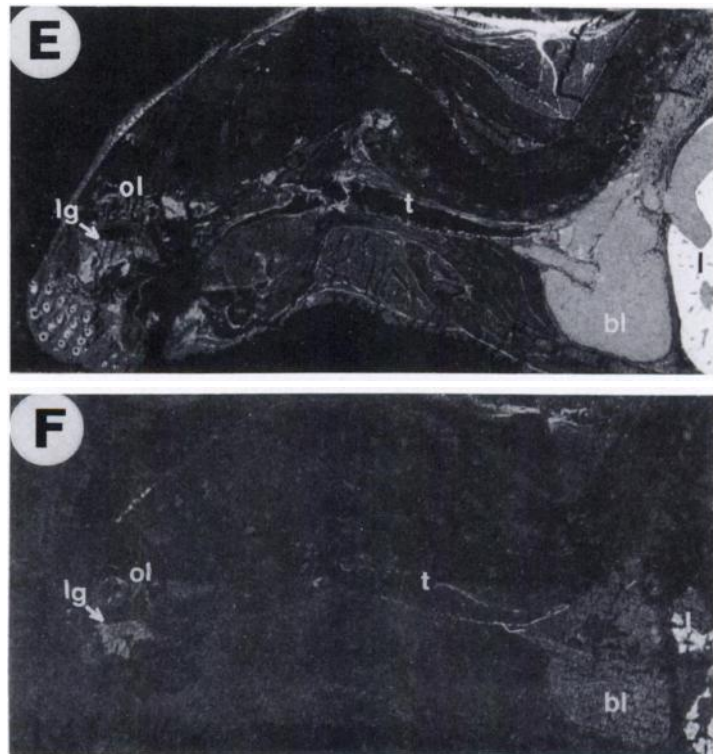

Fig. 1. Whole-body autoradiograms of freeze-dried sections (A, C, E) and adjacent extracted sections (B, D, F) of a phorone-pretreated mouse (C, D and E, F) and a control mouse (A, B) killed 1 h after s.c. injections of ^{3}H-AFB₁ (80 μg/kg body weight). bl, blood; l, liver; lg, lateral nasal gland; ol, nasal olfactory mucosa; re, nasal respiratory mucosa; t, trachea.

nonpretreated mice given injections of the ³H-AFB₁. However, in the phorone-pretreated mice there was a marked, nonextractable labeling of the nasal olfactory and respiratory mucosa, the mucosa of the nasopharyngeal duct and the tracheal mucosa, which was not seen in the nonpretreated mice (Fig. 1, C–F). In these mice there was also a weak labeling of the esophageal mucosa. Similar results were observed in the phorone-pretreated mice given injections of the low and the high doses of the ³H-AFB₁.

In the autoradiograms of freeze-dried tissue sections of the 5- and 1-day-old infants given injections of ³H-AFB₁, there was a labeling of the nasal olfactory mucosa which was not seen in the non-phorone-pretreated adults (Figs. 2A and 3A). The labeling of the liver was somewhat lower in the 1-day-old infant than in the 5-day-old infant and also compared with the adults. In other aspects the distribution patterns were similar in the infants and the adults.

In extracted sections of the infants, a marked radioactivity was retained in the nasal olfactory mucosa and the nasal glands (Figs. 2B and 3B). A considerable radioactivity was retained in the liver of the 5-day-old infant, whereas in the 1-day-old infant

the level of bound radioactivity in the liver was low. In the 5-day-old infant, tissue-bound radioactivity was also retained in the nasal respiratory mucosa, the mucosa of the nasopharyngeal duct, the tracheal mucosa, and the pharyngeal and esophageal mucosa (Fig. 2B). The labeling at these sites was low in the 1-day-old mouse (Fig. 3B).

In autoradiograms of freeze-dried sections of the 18-day-pregnant mice killed 1 and 4 h after the injections of ³H-AFB₁ a low labeling was seen in most fetal tissues. A marked radioactivity was present in the nasal olfactory mucosa and the eye melanin (Fig. 4A). Considerable labeling was also seen in the intestinal contents. The labeling of the fetal liver was low. In extracted sections radioactivity was retained in the nasal mucosa and the eye, but was lost from the other fetal tissues.

In the 14-day-pregnant mouse killed 1 h after the injection of ³H-AFB₁ marked labeling was seen in the fetal eye melanin but was low in all other fetal tissues (Fig. 4C).

Microautoradiography of Tissues of the 5-Day-Old Mouse Given ³H-AFB₁ Injection. Microautoradiography of the nasal olfactory mucosa of the 5-day-old mouse killed 1 h after injection of ³H-AFB₁ showed the highest labeling over Bowman's
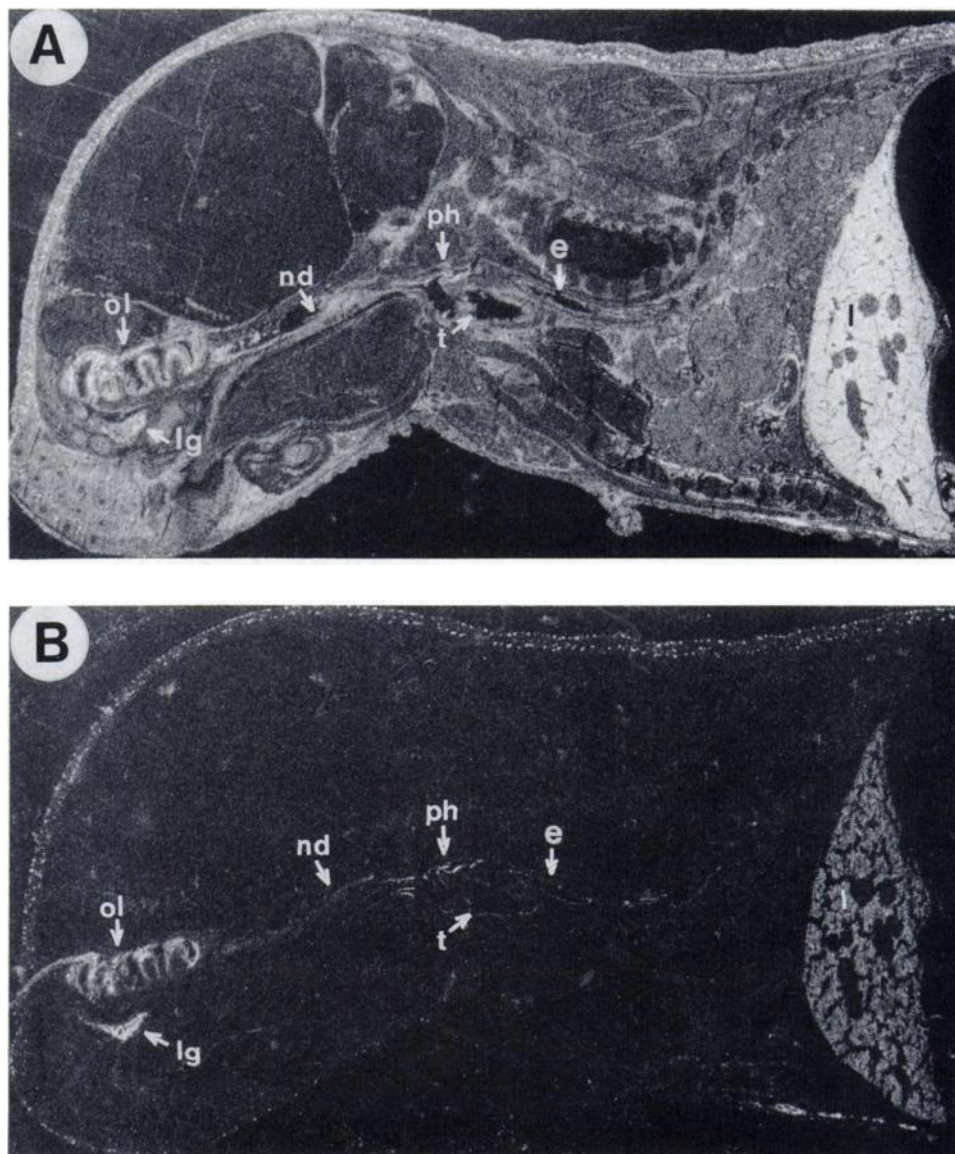

Fig. 2. Whole-body autoradiograms of a freeze-dried section (A) and an adjacent extracted section (B) of a 5-day-old mouse killed 1 h after a s.c. injection of ³H-AFB₁ (80 μg/kg body weight). l, liver; lg, lateral nasal gland; nd, nasopharyngeal duct; e, esophagus; ol, nasal olfactory mucosa; ph, pharynx; t, trachea.
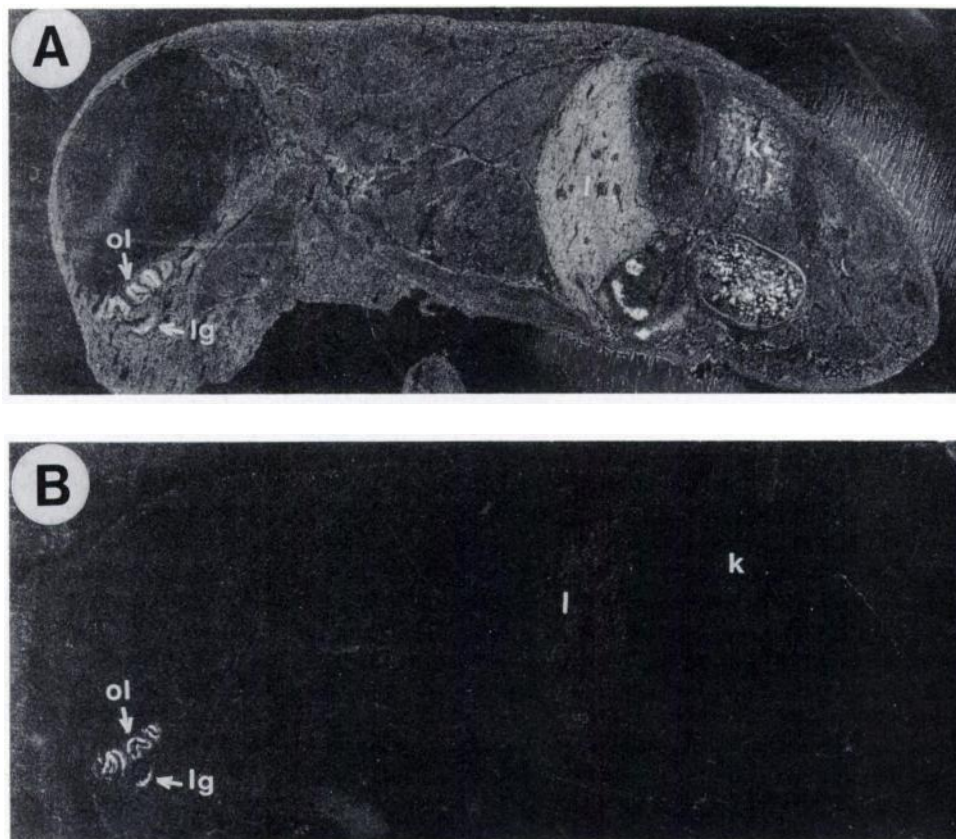
Fig. 3. Whole-body autoradiograms of a freeze-dried section (*A*) and an adjacent extracted section (*B*) of a 1-day-old mouse killed 1 h after a s.c. injection of ³H-AFB₁ (80 μg/kg body weight). *k*, kidney; *l*, liver; *lg*, lateral nasal gland; *ol*, nasal olfactory mucosa.

gland in the lamina propria mucosae (Fig. 5*A*). In addition, a low labeling was seen in the olfactory surface epithelium. In the nasal respiratory mucosa a marked labeling was present in a few serous glands and a somewhat lower radioactivity in the surface epithelium (Fig. 5*B*). In the trachea a few epithelial mucous cells had a moderate radioactivity (Fig. 5*C*). Microautoradiograms of the esophagus showed a distinct labeling of the outer part of the epithelium, whereas the labeling of the middle and basal cell layers was low (Fig. 5*D*).

Microautoradiography of Tissues Incubated with ³H-AFB₁. Microautoradiography of the adult nasal olfactory mucosa incubated with ³H-AFB₁ showed a strong labeling over the nuclei of the sustentacular cells in the surface epithelium (Fig. 6*A*). The neuronal and basal cells were weakly labeled, and this applied also to the cells of Bowman's glands. In the nasal respiratory epithelium there was a strong labeling of the nuclei of the cells in the surface epithelium and a weak labeling of the nuclei of secretory cells of serous glands in the lamina propria mucosae (Fig. 6*B*).

Microautoradiography of the nasal olfactory and respiratory mucosa from the 5-day-old mouse incubated with ³H-AFB₁ showed pictures similar to those for the adult animal (data not shown).

Autoradiography of the Esophagus Incubated with ³H-AFB₁. In autoradiograms of freeze-dried tape sections of the esophagus of the adult mouse, there was a strong labeling of the surface epithelium when the incubation was performed in an O₂ atmosphere (Fig. 7*A*). Other structures, such as the submucosa, the fibrosa, and the muscles, showed a lower labeling. When the incubations were performed in N₂ atmosphere, CO atmosphere, or O₂ atmosphere with metyrapone present in the incubation medium the labeling of the surface epithelium was

lower than when the incubations were performed in the O₂ atmosphere (with no metyrapone in the medium) (Fig. 7*A*). In tissue sections extracted in trichloroacetic acid and organic solvents before the autoradiography a distinct radioactivity was retained in the surface epithelium of the esophagus incubated in O₂ atmosphere (without metyrapone) (Fig. 7*B*). The labeling of the other structures (submucosa, fibrosa, and muscles) was lost from the esophagus incubated in O₂ atmosphere. The extractions removed all labeling in the esophagi incubated with N₂ atmosphere, CO atmosphere, or O₂ atmosphere with metyrapone in the incubation medium (Fig. 7*B*).

Formation of Protein-bound AFB₁ Metabolites by S-9 Preparations of the Nasal Olfactory Mucosa, the Esophageal Mucosa, and the Liver. Incubations of 0.13 μM ³H-AFB₁ with increasing amounts of tissue protein concentrations showed a linear increase of bound radioactivity up to 0.4 mg protein/ml incubation solution (Fig. 8*A*). The highest values were obtained with the adult nasal olfactory mucosa at all protein concentrations. The infant nasal olfactory mucosa showed higher values than the infant liver. For the adult esophageal mucosa the values were lower than for the adult liver. The incubation-time-dependent formation of protein-bound radioactivity was linear up to 30 min for all tissues (data not shown; these incubations were performed with 0.25 mg protein and 0.13 μM ³H-AFB₁).

In the incubations carried out for 20 min, with increasing amounts of AFB₁ and a constant amount of tissue protein (0.25 mg protein), the S-9 preparations of the adult nasal olfactory mucosa were the most effective ones in bioactivating the ³H-AFB₁ to metabolites which bind to the proteins at all concentrations of the ³H-AFB₁ (Fig. 8*B*). The S-9 preparations of the infant nasal olfactory mucosa formed amounts of bound metabolites similar to those for the adult liver. The lowest values
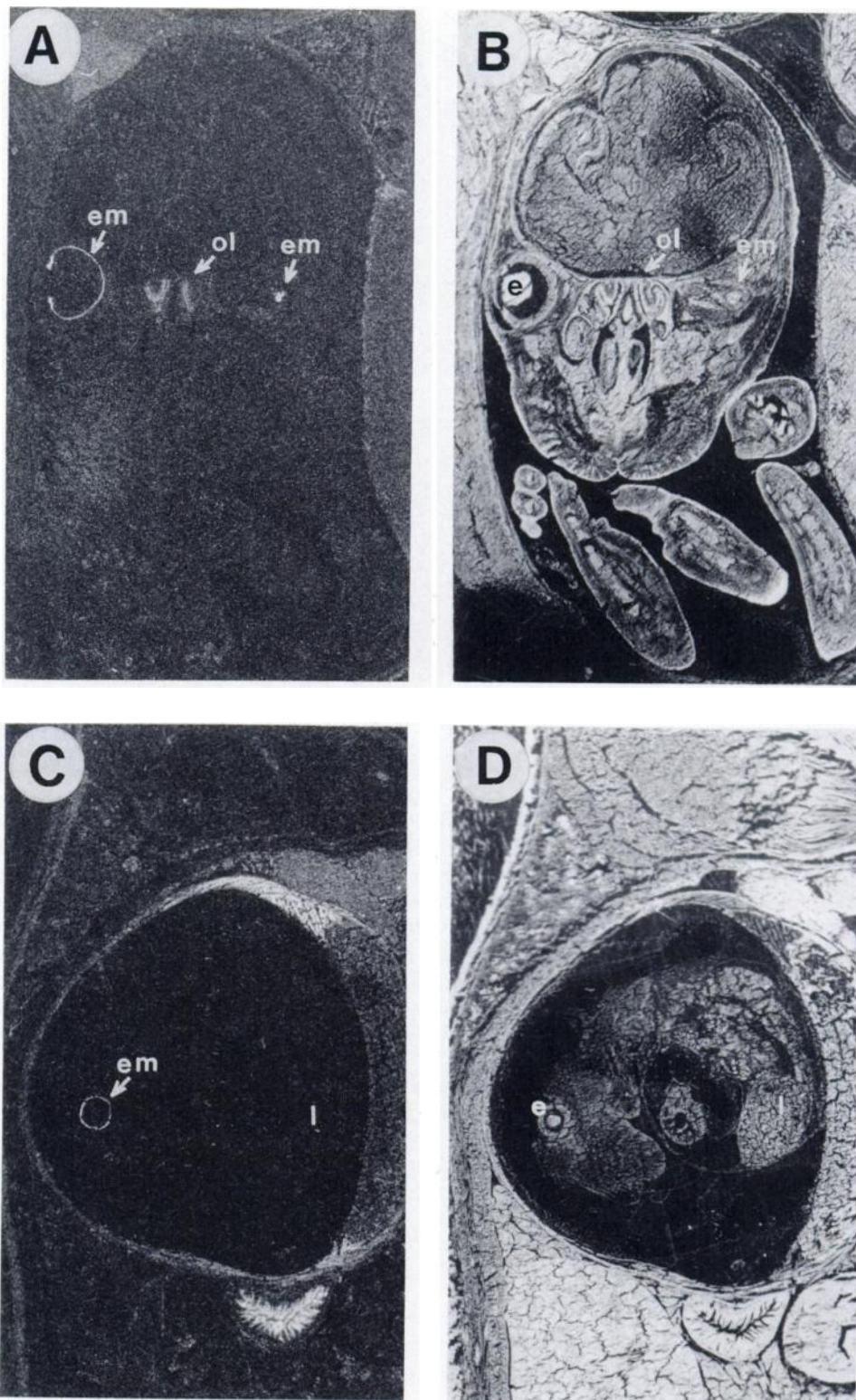
Fig. 4. Details of whole-body autoradiograms (showing fetuses) of freeze-dried sections (*A*, *C*) and the corresponding tissue sections (*B*, *D*) of a 18-day-pregnant mouse (*A*, *B*) and a 14-day-pregnant mouse (*C*, *D*) killed 1 h after i.v. injections of ^{3}H-AFB₁ (42 μg/kg body weight). *e*, eye; *em*, eye melanin; *l*, liver; *ol*, nasal olfactory mucosa.

were observed for the adult esophageal mucosa and the infant liver.

When 5 mM GSH was added to the ^{3}H-AFB₁-incubations the level of protein-bound radioactivity was lowered both in the tissues of the adults and the 5-day-old infants (Table 1). The highest scavenging capacity of the GSH was observed in the adult nasal olfactory mucosa in which the ^{3}H-AFB₁ binding decreased from about 68 to about 18 pmol/mg protein. In the nasal olfactory mucosa of the 5-day-old infant the binding

decreased from about 4 to about 1.2 pmol/mg protein. In the liver the GSH had a higher scavenging capacity in the adult than in the infant mouse. In the adult esophagus the GSH reduced the binding from about 2.2 to about 0.9 pmol/mg protein. The contribution of endogenous GSH in the experiments above can be neglected, since a very rapid decrease in GSH contents takes place in untreated tissue homogenates (18).

Addition of 0.5 mM metyrapone to the incubation media lowered the levels of protein-bound radioactivity to 2% of the
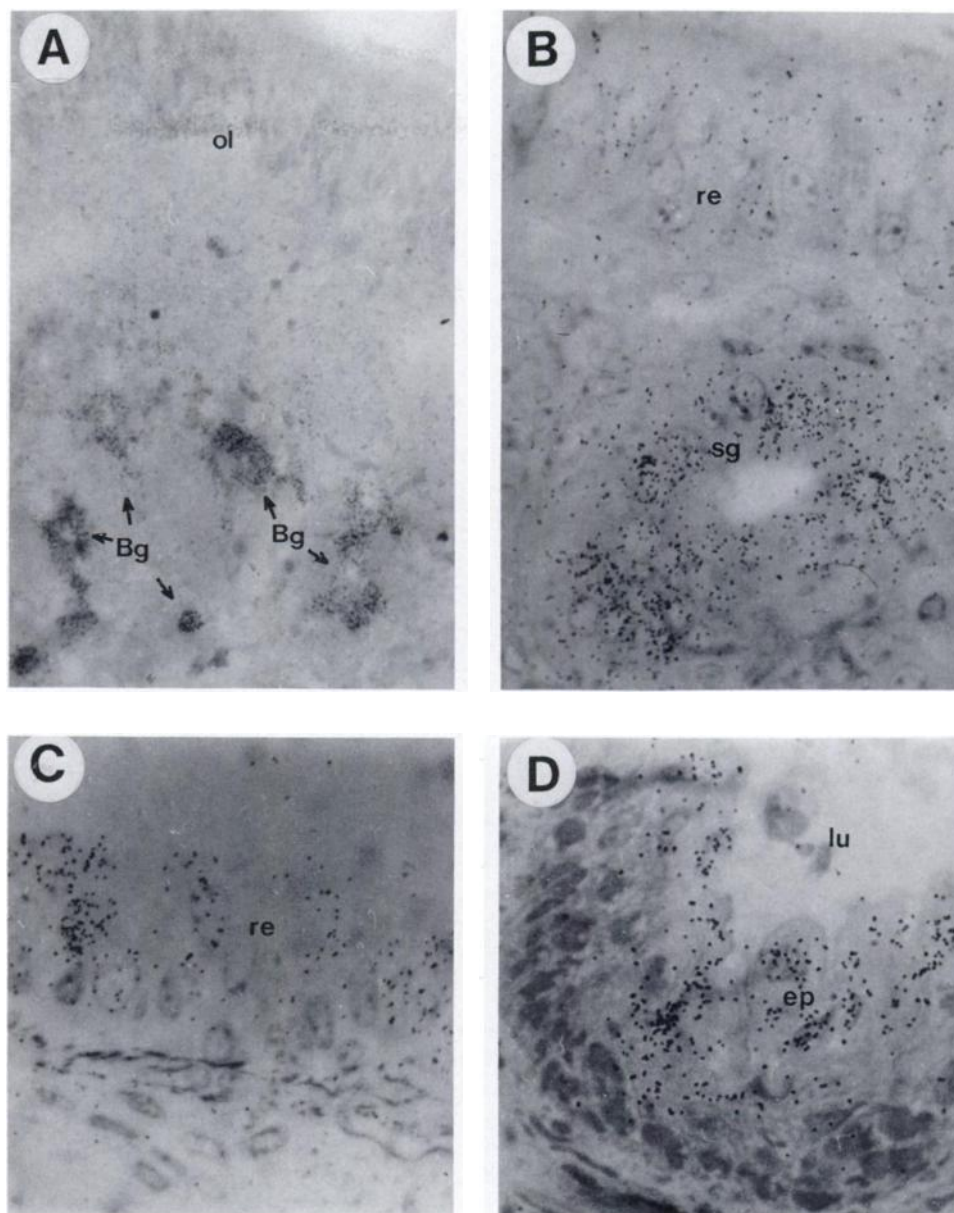
Fig. 5. Microautoradiograms of the nasal olfactory mucosa (A), the nasal respiratory mucosa (B), the trachea (C), and the esophagus (D) from a 5-day-old mouse killed 1 h after a s.c. injection of ³H-AFB₁ (300 μg/kg body weight). Bg, Bowman's glands; ep, esophageal epithelium; lu, esophageal lumen; ol, olfactory epithelium; re, respiratory epithelium; sg, serous gland. A, × 200; B, C, × 350; D, × 400.

control values in the nasal olfactory mucosa and to 36% in the liver.

Effect of Phorone Treatment on NPSH Levels in the Nasal Olfactory Mucosa and the Liver. The NPSH contents were about 2.5 μmol/g wet tissue in the nasal olfactory mucosa, about 3.3 μmol/g wet tissue in the esophageal mucosa, and about 9.4 μmol/g wet tissue in the liver. Two h after administration of phorone, the NPSH levels were strongly lowered in all tissues (Table 2).

DISCUSSION

The results of the present study have shown that the autoradiographic distribution pictures of the ³H-AFB₁ in the phorone-pretreated adult mice differ from those obtained in the unpretreated adult mice. Thus, in the phorone-pretreated mice radioactivity could be seen in the upper respiratory tissues, most markedly in the nasal olfactory mucosa, and in the esophagus, which was not seen in the unpretreated mice. The *in vitro* data

showed a very high capacity of the nasal olfactory mucosa to bioactivate the ³H-AFB₁ (determined as the formation of protein-bound AFB₁ radioactivity). Bioactivation of AFB₁ was also observed in the esophageal mucosa. Incubations in the presence of GSH strongly depressed the formation of protein-bound metabolites in both the nasal olfactory mucosa and the esophageal mucosa.

Our results also showed a strong GSH depletion in the nasal olfactory mucosa and the esophageal mucosa of the adult mice treated with phorone. It has previously been shown that phorone reduces the GSH levels in the liver, kidney, and heart of mice (19). Decreased GSH levels in the liver were observed also in the present study. Phorone has been reported to be without effect on the microsomal mixed function oxidase system or on GST (19, 20).

The altered distribution of ³H-AFB₁ induced by phorone is probably related to decreased tissue levels of GSH. Thus, it is likely that in the non-phorone-pretreated mice given AFB₁, the AFB₁-8,9-epoxide is formed in the extrahepatic tissues but is
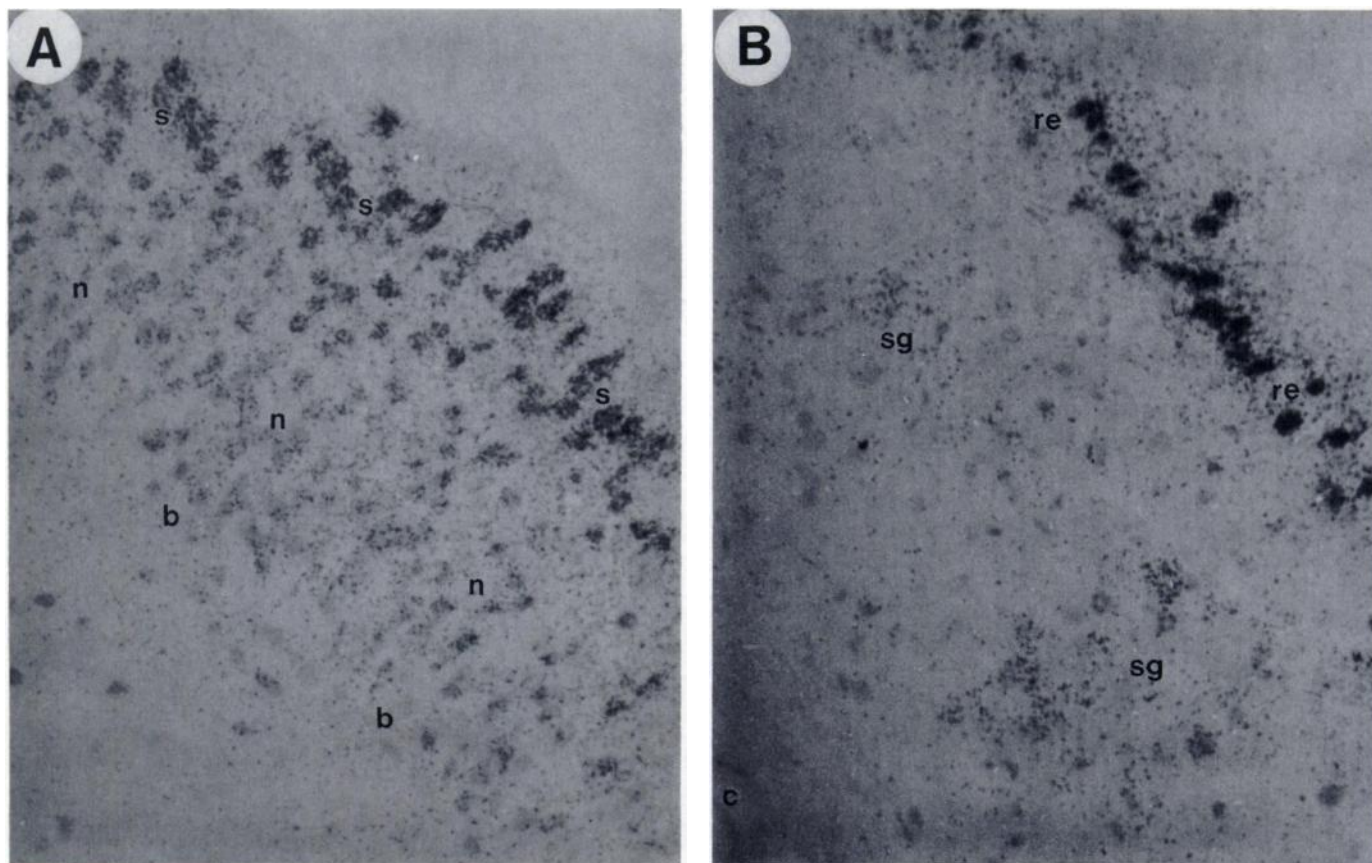
Fig. 6. Microautoradiograms of incubated tissues from an adult mouse showing (*A*) the nasal olfactory mucosa and (*B*) the nasal respiratory mucosa. The tissues were incubated for 1 h in a buffer containing ^{3}H-AFB₁ (0.07 μM). *b*, basal cells; *c*, cartilage; *n*, neuronal cells; *re*, cells of the respiratory surface epithelium; *sg*, cells of serous glands; *s*, sustentacular cells. × 250.

efficiently conjugated with GSH, which prevents binding to tissue macromolecules. When the GSH levels are decreased by phorone treatment, binding to tissue macromolecules will take place.

We have previously reported that, in the nasal cavity of unpretreated mice given injections of ^{3}H-AFB₁, high levels of radioactivity are bound only in the lateral nasal gland (Steno's gland) and certain other nasal glands (14). This was confirmed in the present study. The nasal glands were also shown to have a capacity to form tissue-bound AFB₁ metabolites *in vitro*, and this binding was depressed by GSH, although to a lower extent than observed in the liver (14). It is probable that, in contrast to the other extrahepatic tissues, the GST activity is insufficient in the nasal glands to prevent tissue binding of the AFB₁-8,9-epoxide *in vivo*.

We have previously shown a very high metabolism of AFB₁ in the bovine olfactory mucosa (21). In the present study the *in vitro* microautoradiography showed a strong labeling of the nuclei of the sustentacular cells. This was seen also in bovines (21) and may reflect a specific affinity of bioactivated AFB₁ for DNA (22).

Our autoradiographic data indicated that AFB₁ is metabolized in the tracheal mucosa. *In vitro* metabolism of AFB₁ has been observed in tracheal explants of some species (23).

The *in vitro* autoradiography of the esophagus indicated a metabolism of the ^{3}H-AFB₁ in the epithelial lining of this tissue in the adult mice. The observation that the binding of AFB₁ metabolites to the esophageal epithelium was inhibited by the cytochrome P-450 inhibitor metyrapone and by CO and N₂

atmospheres indicates a cytochrome P-450-dependent bioactivation of the AFB₁ in this tissue. This also applies to the nasal olfactory mucosa, in which the binding of AFB₁ metabolites was strongly depressed by metyrapone.

Cytochrome P-450 enzymes have been shown in the nasal olfactory mucosa and in the epithelial linings of the upper respiratory and alimentary pathways (21, 24-29). These tissues are also prevalent sites for the metabolism of several xenobiotics, such as *N*-nitrosamines and haloalkanes (30). The isoenzyme patterns may differ in the various tissues. In addition, the extrahepatic tissues are heterogeneous, and high cytochrome P-450 activities are confined to specific cell types in the mucosae. In the nasal olfactory mucosa the level of cytochrome P-450 reductase has been reported to be very high (21, 31) and this may promote metabolism.

As mentioned introductorily, the GST activity towards several substrates is low in the liver of young mice (13). This correlates with our findings that the *in vitro* binding of AFB₁ to macromolecules in the liver was more strongly depressed by GSH in adults as compared to 5-day-old infants.

The observation that the nasal olfactory and respiratory mucosa, the tracheal mucosa, and the esophageal mucosa accumulated bound AFB₁ metabolites in the infant mouse may also be related to low GST activity in early life. Our results showed that in the nasal olfactory mucosa the GST activity, estimated as the inhibition of AFB₁ macromolecular binding in the presence of GSH, was much higher in the adults than in infants. The accumulation of bound ^{3}H-AFB₁ metabolites in the esophagus of the 5-day-old infant may also be related to a

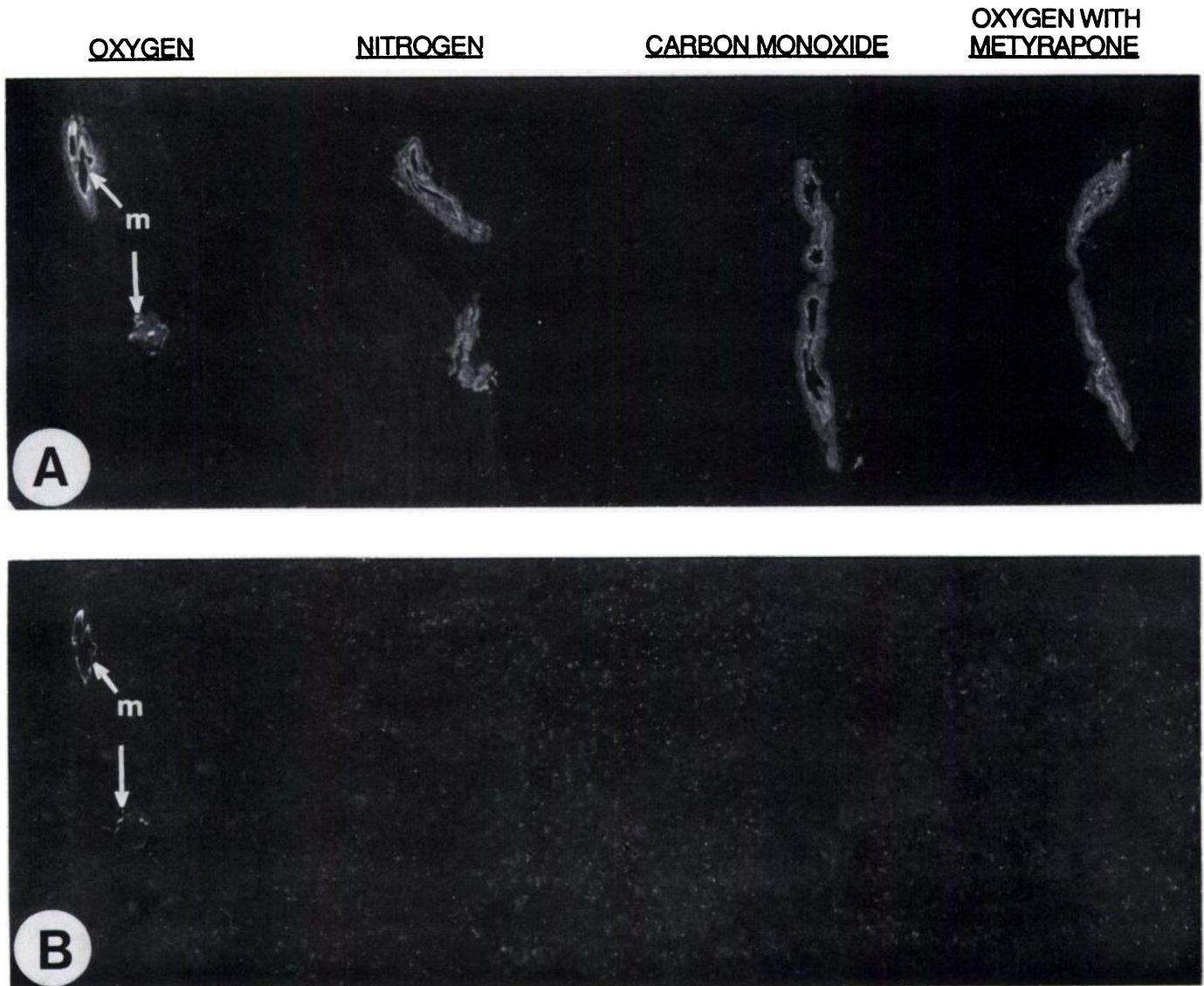OXYGEN	NITROGEN	CARBON MONOXIDE	OXYGEN WITH METYRAPONE

Fig. 7. Autoradiograms of incubated esophagus from adult mice. *A*, autoradiogram of a freeze-dried tape section; *B*, autoradiogram of an extracted tape section. The incubations were carried out for 1 h in a buffer containing ^{3}H-AFB$_1$ (0.07 μM) in O$_2$, N$_2$, CO, or O$_2$ atmosphere with metyrapone (0.5 mM) present in the incubation medium (*top abscissa*). *m*, esophageal mucosa.

considerable AFB$_1$-bioactivating capacity of this tissue in the young animals. The cytochrome P-450-dependent activation of the esophageal carcinogen *N*-nitrosomethylamylamine has been shown to occur to a higher extent in the esophagus in young animals as compared to adults (32).

The microautoradiography of the nose in the 5-day-old mouse given an injection of ^{3}H-AFB$_1$ showed a strong labeling of Bowman's glands, whereas the surface epithelium was labeled to a lower extent. The *in vitro* autoradiography in the 5-day-old infant showed the strongest labeling over the sustentacular cells and, as mentioned previously, the same observation was done in the adult mouse. Thus, the cells in the nose, which will be engaged in AFB$_1$ bioactivation, may vary depending on the route of exposure: AFB$_1$ reaching the nose systemically via the blood may be metabolized mainly in Bowman's glands; local exposure via inhalation may result in metabolism in the sustentacular cells in the surface epithelium, as was seen in our *in vitro* microautoradiography.

In the fetuses bound AFB$_1$ metabolites were seen in the nasal mucosa in the 18-day-pregnant mouse but not in the 14-day-

pregnant mouse. It is probable that the AFB$_1$-bioactivating enzymes in the nasal mucosa do not develop until late in fetal life. Our data also showed a much lower labeling of the liver than of the nasal mucosa in the 18-day-old fetus and in the 1-day-old infant. Similar results have been observed with some *N*-nitrosamines (33). This indicates that some cytochrome P-450 enzymes may develop earlier in the nasal mucosa than in the liver.

AFB$_1$ radioactivity accumulated in the eye melanin in the fetuses as well as in young and adult mice. Melanin has a capacity to bind AFB$_1$ *in vivo* and *in vitro* (34). The labeling of the fetal eye is an indication that considerable quantities of nonmetabolized AFB$_1$ have reached the fetuses.

Labeling of the fetal nasal mucosa and eye melanin has been reported in an earlier autoradiographic study with ^{14}C-labeled AFB$_1$ in mice (35).

Few studies have examined the carcinogenic effectiveness of AFB$_1$ after exposure transplacentally or during early life. In one study, liver tumors were induced by i.p. injections of AFB$_1$ in young mice (36). The low GST activity in the young mice
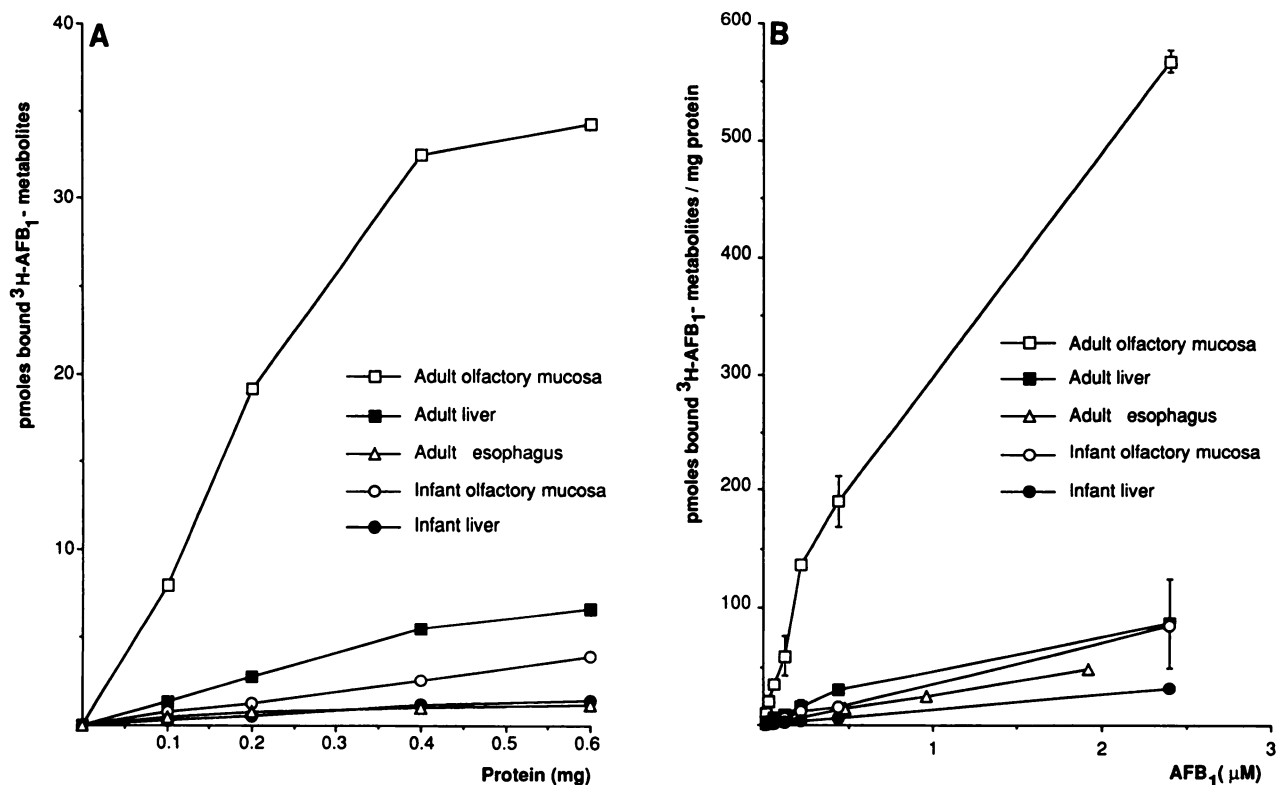
Fig. 8. Formation of protein bound metabolites from ³H-AFB₁ by S-9 preparations of the nasal olfactory mucosa, the esophageal mucosa and the liver. (A) Binding of ³H-AFB₁ metabolites to S-9 protein at various protein concentrations in the incubation media. The incubations were performed for 20 min with 0.13 μM ³H-AFB₁. Each point represents the mean of 2 values. (B) Substrate-concentration-dependent binding of ³H-AFB₁ metabolites to S-9 proteins of the nasal olfactory mucosa, the esophageal mucosa and the liver. The incubations were performed for 20 min with 0.25 mg S-9 proteins. Each point represents the binding expressed as mean ± SD (olfactory mucosa, n = 2; esophageal mucosa, n = 2; infant liver, n = 3; adult liver, n = 6).

Table 1 Effects of GSH (5 mM) on the formation of protein-bound metabolites by S-9 preparations of tissues from adult and 5-day-old infant mice

Incubations were performed for 20 min with 0.25 mg S-9 protein and 0.08 μM ³H-AFB₁. Mean ± SD (n = 3 in all cases except the adult nasal olfactory mucosa, for which n = 4).

	Amounts of ³H-AFB₁ metabolites bound (pmol/mg protein)	
Tissue	A. Without GSH	B. With GSH
Adult		
Nasal olfactory mucosa	67.9 ± 2.0	17.8 ± 1.9[a]
Esophageal mucosa	2.2 ± 0.1	0.9 ± 0.1[a]
Liver	8.8 ± 1.9	1.2 ± 0.3[b]
Infant		
Nasal olfactory mucosa	4.0 ± 1.1	1.2 ± 0.5[c]
Liver	2.7 ± 0.2	0.8 ± 0.1[a]

[a] Significantly different from A, P < 0.001.
[b] Significantly different from A, P < 0.05.
[c] Significantly different from A, P < 0.01.

Table 2 Effect of phorone on the contents of non-protein sulfhydryl groups (NPSH) in tissues of adult mice.

Groups of mice were given phorone (250 mg/kg body weight; dissolved in corn oil) i.p., or corn oil only (controls) and were killed after 2 h. The results are expressed as mean values (with the range within parentheses) from pooled samples of two groups of control and two groups of phorone-treated mice. All values for the phorone-treated mice differ significantly from the controls (P < 0.001).

	NPSH contents (μmol/g wet tissue)	
Tissue	Control	Phorone-treated
Nasal olfactory mucosa	2.5 (0.4)	0.5 (0.1)
Esophageal mucosa	3.3 (0.2)	0.5 (0.2)
Liver	9.4 (0.6)	0.7 (0.1)

may contribute to their sensitivity, but additional factors, such as bioactivating ability, rates of cell replication, and repair of DNA lesions may also be involved. As mentioned previously, adult mice appear to be refractory to the carcinogenic actions of this compound.

The respiratory tissues have not been reported to be targets for AFB₁ carcinogenicity in mice. However, nasal and tracheal tumors have been reported in rats exposed to AFB₁ transplacentally or during early postnatal life (37).

Extended studies on the carcinogenicity of AFB₁ at exposure during fetal or early postnatal life would be of interest. Conceivably, extrahepatic tissues may be more sensitive to carcinogenesis at exposure during these periods of life, due to factors such as early development of bioactivating capacity and insufficient ability to detoxify reactive metabolites.

ACKNOWLEDGMENTS

REFERENCES

1. Swenson, D. H., Miller, E. C., and Miller, J. A. Aflatoxin B₁-2,3-oxide: evidence for its formation in rat liver in vivo and by human liver microsomes in vitro. Biochem. Biophys. Res. Commun., 60: 1036–1043, 1974.
2. Swenson, D. H., Lin, J-K., Miller, E. C., and Miller, J. A. Aflatoxin B₁-2,3-oxide as a probable intermediate in the covalent binding of aflatoxins B₁ and B₂ to rat liver DNA and ribosomal RNA in vivo. Cancer Res., 37: 172–181, 1977.
3. Essigmann, J. M., Croy, R. G., Bennett, R. A., and Wogan, G. N. Metabolic activation of aflatoxin B₁: patterns of DNA adduct formation, removal and excretion in relation to carcinogenesis. Drug Metab. Rev., 13: 581–602, 1982.
4. Degen, G. H., and Neumann, H-G. The major metabolite of aflatoxin B₁ in the rat is a glutathione conjugate. Chem.-Biol. Interact., 22: 239–255, 1978.

5. Emerole, G. O., Neskovic, N., and Dixon, R. L. The detoxication of aflatoxin B₁ with glutathione in the rat. Xenobiotica, 9: 737–743, 1979.
6. Neal, G. E., and Green, J. A. The requirement for glutathione S-transferase in the conjugation of activated aflatoxin B₁ during aflatoxin hepatocarcinogenesis in the rat. Chem.-Biol. Interact., 45: 259–275, 1983.
7. Neal, G. E., and Colley, P. J. The formation of 2,3-dihydro-2,3-dihydroxy aflatoxin B₁ by the metabolism of aflatoxin B₁ in vitro by rat liver microsomes. FEBS Lett., 101: 382–386, 1979.
8. Hsieh, D. P. H. Biological reactive intermediates of mycotoxins. Adv. Exp. Med. Biol., 197: 597–610, 1986.
9. Monroe, D. H., and Eaton, D. L. Comparative effects of butylated hydroxyanisole on hepatic in vivo DNA binding and in vitro biotransformation of aflatoxin B₁ in the rat and mouse. Toxicol. Appl. Pharmacol., 90: 401–409, 1987.
10. Neal, G. E., Nielsch, U., Judah, D. J., and Hulbert, P. B. Conjugation of model substrates of microsomally-activated aflatoxin B₁ with reduced glutathione, catalysed by cytosolic glutathione-S-transferases in livers of rats, mice and guinea pigs. Biochem. Pharmacol., 36: 4269–4276, 1987.
11. Ramsdell, H. S., and Eaton, D. L. Mouse liver glutathione S-transferase isoenzyme activity toward aflatoxin B₁-8,9-epoxide and benzo[a]pyrene-7,8-dihydrodiol-9, 10-epoxide. Toxicol. Appl. Pharmacol., 105: 216–225, 1990.
12. Quinn, B. A., Crane, T. L., Kocal, T. E., Best, S. J., Cameron, R. G., Rushmore, T. H., Farber, E., and Hayes, M. A. Protective activity of different hepatic cytosolic glutathione S-transferases against DNA-binding metabolites of aflatoxin B₁. Toxicol. Appl. Pharmacol., 105: 351–363, 1990.
13. Gregus, Z., Varga, F., and Schmelás, A. Age-development and inducibility of hepatic glutathione S-transferase activities in mice, rats, rabbits and guinea-pigs. Comp. Biochem. Physiol., 80C: 85–90, 1985.
14. Larsson, P., Hoedaya, W. I., and Tjälve, H. Disposition of ³H-aflatoxin B₁ in mice: formation and retention of tissue bound metabolites in nasal glands. Pharmacol. Toxicol., 67: 162–171, 1990.
15. Ullberg, S. The technique of whole body autoradiography: cryosectioning of large specimens. Science Tools. pp. 2–29. In: The LKB Instrument Journal, Special Issue on Whole Body Autoradiography, 1977.
16. Baker, M. T., and Van Dyke, R. A. Metabolism dependent binding of the chlorinated insecticide DDT and its metabolite DDD to microsomal proteins and lipids. Biochem. Pharmacol., 43: 255–260, 1984.
17. Lowry, O. H., Rosebrough, N. J., Farr, A. L., and Randall, R. J. Protein measurement with the Folin phenol reagent. J. Biol. Chem., 193: 265–275, 1951.
18. Sedlak, J., and Lindsay, R. H. Estimation of total, protein-bound and nonprotein sulfhydryl groups in tissue with Ellman's reagent. Anal. Biochem., 25: 192–205, 1968.
19. Younes, M., Sharma, S. C., and Siegers, C-P. Glutathione depletion by phorone. Organ specificity and effect on hepatic microsomal mixed-function oxidase system. Drug Chem. Toxicol., 9: 67–73, 1986.
20. Siegers, C-P., Hübscher, W., and Younes, M. Glutathione-S-transferase and GSH-peroxidase activities during the state of GSH-depletion leading to lipid peroxidation in rat liver. Res. Commun. Chem. Pathol. Pharmacol., 37: 163–169, 1982.
21. Larsson, P., Pettersson, H., and Tjälve, H. Metabolism of aflatoxin B₁ in the bovine olfactory mucosa. Carcinogenesis (Lond.), 10: 1113–1118, 1989.
22. Misra, R. P., Muench, K. F., and Humayun, M. Z. Covalent and noncovalent interactions of aflatoxin with defined deoxyribonucleic acid sequences. Biochemistry, 22: 3351–3359, 1983.
23. Wilson, D. W., Ball, R. W., and Coulombe, R. A., Jr. Comparative action of aflatoxin B₁ in mammalian airway epithelium. Cancer Res., 50: 2493–2498, 1990.
24. Dahl, A. R., Hadley, W. M., Hahn, F. F., Benson, J. M., and McClellan, R. O. Cytochrome P-450-dependent monooxygenases in the olfactory epithelium of dogs: Possible role in tumourigenicity. Science (Washington DC), 216: 57–59, 1982.
25. Labuc, G. E., and Archer, M. C. Esophageal and hepatic microsomal metabolism of N'-nitrosomethylbenzylamine and N-nitrosodimethylamine in the rat. Cancer Res., 42: 3181–3186, 1982.
26. Voigt, J. M., Guengerich, F. P., and Baron, J. Localization of a cytochrome P-450 isozyme (cytochrome P-450 PB-B) and NADPH-cytochrome P-450 reductase in rat nasal mucosa. Cancer Lett., 27: 241–247, 1985.
27. Baron, J., Burke, J. P., Guengerich, F. P., Jakoby, W. B., and Voigt, J. M. Sites for xenobiotic activation and detoxication within the respiratory tract: implications for chemically induced toxicity. Toxicol. Appl. Pharmacol., 93: 493–505, 1988.
28. Ding, X., and Coon, M. J. Purification and characterization of two unique forms of cytochrome P-450 from rabbit nasal microsomes, Biochemistry, 27: 8330–8337, 1988.
29. Reed, C. J., Lock, E. A., and De Matteis, F. Olfactory cytochrome P-450. Studies with suicide substrates of the haemoprotein. Biochem. J., 253: 569–576, 1988.
30. Tjälve, H. Tissue-specificity of N-nitrosamine-metabolism in experimental animals: Studies on some N-nitrosamines present in tobacco and tobacco smoke. In: A. P. Maskens et al. (eds.), Tobacco and Cancer. Perspectives in Preventive Research, pp. 5–21, Amsterdam: Elsevier Science Publishers B. V., Biomedical Division, 1985.
31. Reed, C. J., Lock, E. A., and De Matteis, F. NADPH: cytochrome P-450 reductase in olfactory epithelium. Relevance to cytochrome P-450-dependent reactions. Biochem. J., 240: 585–592, 1986.
32. Mirvish, S. S., Ji, C., and Rosinsky, S. Hydroxy metabolites of methyl-n-amylnitrosamine produced by esophagus, stomach, liver and other tissues of the neonatal to adult rat and hamster. Cancer Res., 48: 5663–5668, 1988.
33. Tjälve, H., Löfberg, B., Castonguay, A., Trushin, N., and Hecht, S. S. Perinatal disposition and metabolism in mice and hamsters of some N-nitrosamines present in tobacco and tobacco smoke. Banbury Rep., 23: 179–195, 1986.
34. Larsson, P., Larsson, B. S., and Tjälve, H. Binding of aflatoxin B₁ to melanin. Food Chem. Toxicol., 26: 579–586, 1988.
35. Arora, R. G., Appelgren, L-E., and Bergman, A. Distribution of [¹⁴C]labelled aflatoxin B₁ in mice. Acta Pharmacol. Toxicol., 43: 273–279, 1978.
36. Vesselinovitch, S. D., Mihailovich, N., Wogan, G. N., Lombard, L. S., and Rao, K. V. N. Aflatoxin B₁, a hepatocarcinogen in the infant mouse. Cancer Res., 32: 2289–2291, 1972.
37. Goerttler, K., Löhrke, H., Schweizer, H-J., and Hesse, B. Effects of aflatoxin B₁ on pregnant inbred Sprague-Dawley rats and their F₁ generation. A contribution to transplacental carcinogenesis. J. Natl. Cancer Inst., 64: 1349–1354, 1980.